Springer

Journal of
Mechanical
Science and
Technology

Journal of Mechanical Science and Technology 23 (2009) 3179~3190

www.springerlink.com/content/1738-494x
DOI 10.1007/s12206-009-0919-x

A mathematical model for smart functionally graded beam integrated with shape memory alloy actuators †

H. Sepiani[1,*], F. Ebrahimi[1] and H. Karimipour[2]

[1]*Department of Mechanical Engineering, Faculty of Engineering, University of Tehran, Tehran, Iran*
[2]*Department of Mechanical Engineering, Iran University of Science and Technology, Tehran, Iran*

(Manuscript Received January 27, 2009; Revised June 16, 2009; Accepted August 8, 2009)

Abstract

This paper presents a theoretical study of the thermally driven behavior of a shape memory alloy (SMA)/FGM actuator under arbitrary loading and boundary conditions by developing an integrated mathematical model. The model studied is established on the geometric parameters of the three-dimensional laminated composite box beam as an actuator that consists of a functionally graded core integrated with SMA actuator layers with a uniform rectangular cross section. The constitutive equation and linear phase transformation kinetics relations of SMA layers based on Tanaka and Nagaki model are coupled with the governing equation of the actuator to predict the stress history and to model the thermo-mechanical behavior of the smart shape memory alloy/FGM beam. Based on the classical laminated beam theory, the explicit solution to the structural response of the structure, including axial and lateral deflections of the structure, is investigated. As an example, a cantilever box beam subjected to a transverse concentrated load is solved numerically. It is found that the changes in the actuator's responses during the phase transformation due to the strain recovery are significant.

Keywords: Shape memory alloy (SMA); Functionally graded material (FGM); Smart actuator beam; Classical laminated beam theory (CLBT)

1. Introduction

A new class of materials known as functionally graded materials (FGMs) has emerged recently, in which the material properties vary continuously throughout the continuum and specifically in the plates along the thickness direction. In an effort to develop super heat-resistant materials, Koizumi [1] first proposed the concept of FGMs which are typically made from a mixture of ceramics and metals and are further characterized by a smooth and continuous change of the mechanical properties from one characteristic surface to the other. The ceramic constituents of the FGMs are able to withstand high temperature environments due to their better thermal resistance, while the metal constituents provide stronger mechanical performance and reduce the possibility of catastrophic fracture. Due to their superior thermo-mechanical properties, FGMs have been extensively applied in various industries with high temperature environments.

The laminated composite structures can be tailored to design advanced structures, but the sharp change in the properties of each layer at the interface between two adjacent layers causes large interlaminar shear stresses that may eventually give rise to the well known phenomenon of delamination. Such detrimental effects can be mitigated by grading the properties in a continuous manner across the thickness direction. For example, Teymur et al. [2] carried out a thermo-mechanical analysis of materials, which are functionally graded in two directions, and demonstrated that

† This paper was recommended for publication in revised form by Associate Editor Maenghyo Cho

*Corresponding author. Tel.: +98 912 236 3620, Fax.: +98 21 8801 3029
E-mail address: sepiani@ut.ac.ir

the onset of delamination could be prevented by tailoring the microstructures of the composite plies. Thus, the use of FGMs may become an important issue for developing advanced structures and intensive research has been already reported on the buckling analysis (Feldman and Aboudi [3]), exact solutions (Sankar [4], Batra and Vel [5], Zhong and Shang [6]), dynamic analysis (Loy et al. [7], Yang and Shen [8]) and nonlinear thermo-elastic analysis of structures made of FGM (Woo and Meguid [9], Shen [10]), but the works related to the monitoring and vibration control of FGM structures are limited, namely, the works of Aydogdu and Taskin in presenting Navier type solution method for the vibration of simply supported FGM beam, using Hamilton's principle [11], Zhong and Yu in improving a general two-dimensional solution for a cantilever FGM beam [12], and Sina et al. analyzing the free vibration of FGM beams by means of new theory [13].

In addition to FGMs, over the last four decades or so, a great number of researches have been proposed in the literature in order to investigate the behavior of shape memory alloys. Many researchers have conducted investigations of the basic performance and application of shape memory alloys (SMAs). Therefore, there have been many results of research on SMAs [14–19]. A general 3-D multivariant micromechanical model for shape memory alloy constitutive behavior was developed by Gao et al. [14-16]. Brinson et al. [17] studied the evolution of temperature and deformation profiles seen in SMA wires under specific thermal and mechanical boundary conditions using a macro-scale phenomenological constitutive model for shape memory alloys in conjunction with energy balance equations. She also developed a nonlinear finite element procedure which incorporates a thermo-dynamically derived constitutive law for SMA material behavior [18]. Brocca et al. [19] proposed a model for the behavior of polycrystalline memory alloys, based on a statically constrained microplane theory.

As is well known, if the alloy is trained to have a particular shape in austenite phase, it is capable of remembering this shape. A large plastic deformation can be produced when the alloy is subjected to external force due to martensite transformation. If it is then heated above the austenite transformation temperature and restrained to contract, a large recovery force arises out of the phase transformation from martensite to austenite. Because of this unique property, SMA is prospective in many exciting and innovative engineering applications such as structural vibration control, buckling control and shape control.

In the quest for developing lightweight high performing flexible structures, a concept emerged to develop structures with self-controlling and self-monitoring capabilities. Expediently, these capabilities of a structure were achieved by exploiting the converse and direct innate effects of smart materials as distributed actuators or sensors, which are mounted or embedded in the structure [20-22]. Therefore, advances in design and manufacturing technologies have greatly enhanced the use of advanced composite materials for aircraft and aerospace structural applications. Due to their structural advantages of high stiffness-to-weight and strength-to-weight ratios, composite materials can be used in the design of smart structures and hence significantly improve the performance of aircraft and space structures. In recent years, some researchers have studied shape memory alloy composites (SMACs), which consist of SMA reinforcement and a metal or polymer matrix [23–30]. In particular, considerable attention has been paid to development of several analytical and numerical models for the laminated composite structures with integrated SMA sensors and actuators. Lagoudas et al. [23] and Kawai et al. [41] proposed the constitutive equation of SMAC to predict its mechanical behavior. The present authors [25] reported the fracture behavior under uniaxial tension and the deformation behavior under thermo-mechanical loading on NiTi fiber-reinforced polycarbonate composites. Khalili et al [26, 27] investigated the effect of some important parameters on low-velocity impact response of the active thin-walled hybrid composite plates embedded with the shape memory alloy wires, employing the first-order shear deformation theory as well as the Fourier series method. Sepiani and Ghazavi presented a thermo-micro-mechanical model for studying elastic behavior of woven plain composites embedded with SMA fibers [28]. Zhou et al. [29] Investigated through-the-thickness mechanical properties of smart quasi-isotropic carbon/epoxy laminates and Dano et al. [30] developed a theory and designed experiments to study the concept of using shape memory alloy wires to effect the snap-through of unsymmetric composite laminates. Ghomshei et al. [31, 32] presented a mathematical model for analysis of a thermally driven shape memory alloy/elastomer actuator under arbitrary loading and boundary conditions.

Balapgol et al. [33] studied the free vibration analysis of an SMA surface laminated composite cantilever plate by means of a finite-element method. Chen and Levy [34] proposed the mathematical model of a flexible beam covered with SMA layers.

Although the laminated composite structures with integrated SMA elements have been taken up by many of the aforementioned researchers, to the authors' best knowledge no researches dealing the modeling of FGM structures embedded with smart shape memory alloy layers have been reported in the literature, thus motivating the authors to present a theoretical model to study the thermally driven behavior of an SMA/FGM actuator under arbitrary loading and boundary conditions by developing an integrated mathematical model.

The model studied in this research is established on the geometric parameters of the three-dimensional laminated composite box beam as an actuator that consists of FGM core and SMA bonding layers with a uniform rectangular cross section (Fig. 1). The constitutive equation and linear phase transformation kinetics relations of SMA layers depicted by Tanaka and Nagaki are coupled with the governing equation of the actuator to predict the stress history in smart SMA/FGM beam and to model the thermomechanical behavior. Based on the classical laminated beam theory, the explicit solution to the structural response of the structure, including axial and lateral deflections of the structure, is investigated. As an example, a cantilever box beam with uniform square cross-section subjected to a transverse concentrated load is solved numerically. The effect of some parameters such as activation temperature, FGM layer thickness and FGM index factor is investigated.

2. FG and SMA materials

2.1 Functionally Graded Materials (FGM)

Several available analytical and computational models have discussed the issue of finding suitable functions for material properties, and there are several criteria for selecting them. They should be continuous, simple and have the ability to exhibit curvature, both concave upward and concave downward [35]. In this study the simple power law, which has all the desired properties, is used. Nowadays not only can FGM be easily produced but also one can control even the variation of the FG constituents in a specific way. For example in an FG material made of a ceramic and metal mixture, we have

$$V_m + V_c = 1 \tag{1}$$

in which V_c and V_m are the volume fraction of the ceramic and metallic part, respectively. Based on the power law distribution [36], the variation of V_c versus thickness coordinate (z) with its origin placed at the middle of the thickness can be expressed as

$$V_c = (z/h_2 + 1/2)^g, \quad g \geq 0 \tag{2}$$

in which h_2 is the FG core plate thickness and g is the FGM volume fraction index (see Fig. 1). Note that the variation of both the ceramics and metal constituents is linear when $g = 1$. Moreover, for the value of $g = 0$, a fully ceramic plate is intended. All other mechanical, physical and thermal properties of FGM media follow the same distribution as for V_c. We assume that the inhomogeneous material properties, such as the modulus of elasticity E, the density ρ, thermal expansion coefficient, and thermal diffusivity k, change within the thickness direction z based on Voigt's rule over the whole range of the volume fraction [37] as follows, while Poisson's ratio υ is assumed to be constant in the thickness direction [38] as

$$\begin{aligned} E(z) &= (E_c - E_m)V_c(z) + E_m \\ \rho(z) &= (\rho_c - \rho_m)V_c(z) + \rho_m \\ \alpha(z) &= (\alpha_c - \alpha_m)V_c(z) + \alpha_m \\ k(z) &= (k_c - k_m)V_c(z) + k_m \\ \nu(z) &= \nu \end{aligned} \tag{3}$$

where the subscripts m and c refer to the metal and ceramic constituents, respectively. After substituting V_c from Eq. (2) into Eq. (3), material properties of the FGM beam can be determined in the power law form which are the same as those proposed by Reddy and Praveen [36], i.e.,

$$\begin{aligned} E(z) &= (E_c - E_m)(z/h_2 + 1/2)^g + E_m \\ \rho(z) &= (\rho_c - \rho_m)(z/h_2 + 1/2)^g + \rho_m \\ &\text{etc.} \end{aligned} \tag{4}$$

Contrary to most published papers on FG beams, in this paper we choose a beam with the upper part as being metallic and the lower part as ceramic. This makes us exchange the subscript m in Eq. (4) with c and vice versa. In this way, when $g = 0$ the FG beam

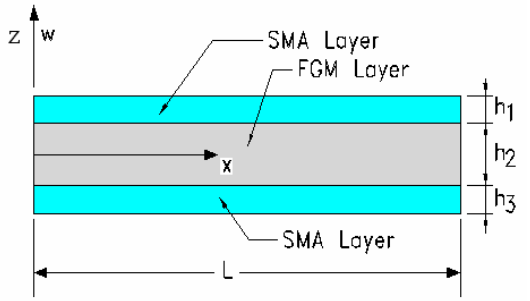

Fig. 1. A schematic illustration of the shape memory alloy/ FGM actuator beam.

becomes completely a metallic isotropic beam. The stress–strain relations for the FGM are similar to those of isotropic beams.

2.2 Shape memory alloy actuators

During martensitic transformation of SMA, the bulk of the metal is uniformly blended with the martensite and austenite phases. The stresses in the SMA layer during this phase transformation are formulated using a 'variable sub-layer' model [39] as follows:

$$\sigma_x(\zeta) = (1-\zeta)\sigma_x^A + \sigma_x^M \tag{5}$$

where ζ is the martensite fraction of SMA during phase transformation. Stress-Strain equation in 3-D applications can be presented in matrix form as

$$\{\sigma(\zeta)\} = [D_{SMA}]\{\varepsilon\} \tag{6}$$

where $[D_{SMA}]$ is the constitutive matrix for the SMA layer. Young's modulus of SMA layer is given by

$$E(\zeta) = (1-\zeta)E_A + \zeta E_M \tag{7}$$

3. Method

The geometrical configuration of the proposed SMA/FGM beam is shown in Fig. 1. SMA layers are assumed to be isolated from each other, so that each one can be activated separately. External faces of actuator, i.e., the outward sides of the SMA layers are in contact with a heat sink with a constant temperature, T_0. It is also assumed that only the upper and the lower SMA layers can be activated simultaneously. Therefore, the beam displacements, including an axial displacement and a lateral deflection, occur only in a plane orthogonal to the activated faces of actuator (xz plane in Fig. 1).

We assume the temperatures in top and bottom SMA layers, T_1 and T_3, are constant, so the temperatures at the upper interface and lower interface of the FGM and SMA layers will be T_1 and T_3, respectively. Neglecting the longitudinal heat conduction, the temperature distribution inside the beam section is determined by solving the 1D unsteady heat conduction problem

$$\frac{\partial T(z,t)}{\partial t} = \frac{\partial}{\partial z}\left(k(z)\frac{\partial T(z,t)}{\partial z}\right) \tag{8}$$

Under the steady-state condition, the above relation is equal to zero. Under the boundary and initial conditions

$$\begin{aligned} &T(z,t) = T_1 && at\ z = h_2/2 \\ &T(z,t) = T_3 && at\ z = -h_2/2 \\ &T(x,t) = T_0 && when\ t = 0 \end{aligned} \tag{9}$$

where T_0 is the initial temperature. The temperature distribution, when assuming steady-state condition, within the FGM part of the beam along the z-coordinate is found to be:

$$\begin{aligned} T_2(z) = T_3 + \frac{\Delta T}{C}\Bigg[&\left(\frac{2z+h_2}{2h_2}\right) - \frac{(k_c-k_m)}{(g+1)k_m}\left(\frac{2z+h_2}{2h_2}\right)^{g+1} \\ &+ \frac{(k_c-k_m)^2}{(2g+1)k_m^2}\left(\frac{2z+h_2}{2h_2}\right)^{2g+1} - \frac{(k_c-k_m)^3}{(3g+1)k_m^3}\left(\frac{2z+h_2}{2h_2}\right)^{3g+1} \\ &+ \frac{(k_c-k_m)^4}{(4g+1)k_m^4}\left(\frac{2z+h_2}{2h_2}\right)^{4g+1} - \frac{(k_c-k_m)^5}{(5g+1)k_m^5}\left(\frac{2z+h_2}{2h_2}\right)^{5g+1}\Bigg] \end{aligned} \tag{10}$$

In which

$$\begin{aligned} C = 1 &- \frac{(k_c-k_m)}{(g+1)k_m} + \frac{(k_c-k_m)^2}{(2g+1)k_m^2} \\ &- \frac{(k_c-k_m)^3}{(3g+1)k_m^3} + \frac{(k_c-k_m)^4}{(4g+1)k_m^4} \\ &- \frac{(k_c-k_m)^5}{(5g+1)k_m^5} \end{aligned} \tag{11}$$

and $\Delta T = T_1 - T_3$ is defined as the temperature difference between metal-rich and ceramic-rich surface

of the plate. Note that the temperature variations along the length and width of the actuator are considered to be negligible. In this study, the classical laminated beam theory is implemented in which the strain field is given by

$$\varepsilon = \varepsilon^0 + z\kappa \tag{12}$$

where

$$\varepsilon^0 = u_{2,x}\ , \qquad \kappa = -w_{,xx} \tag{13}$$

and u_2 and w are axial and lateral displacements of neutral axis of the beam, respectively. The effective axial force N^E and effective bending moment M^E can be expressed as

$$N^E = A\varepsilon^0 + B\kappa, \qquad M^E = B\varepsilon^0 + D\kappa \tag{14}$$

where A, B and D are extensional stiffness, coupling stiffness, and bending stiffness of the beam (actuator) respectively, are given by Gibson [40]

$$\begin{aligned}(A,B,D) = &\int_{A_1+A_2+A_3} E(1,z,z^2)\,dA = \\ &\int_{A_2} E(z)(1,z,z^2)\,dA + \int_{A_1+A_3} E(T,\zeta)(1,z,z^2)\,dA\end{aligned} \tag{15}$$

Here A is cross section area and subscripts *1*, *2* and *3* refer to top layer, core and bottom layer, respectively. Young's modulus of FG material is a complicated function of temperature, but can be approximated by a linear function of T

$$E_2(T,z) = S(T_2 - T_0) + E_0(z) \tag{16}$$

In which S is the slope of change of the FGM's elastic modulus with temperature. Substituting T_2 from Eq. (10) into Eq. (16), one can express the modulus of the FGM layer, as functions of the z coordinate.

Then, we need explicit expressions to be determined for SMA layers' modulus of elasticity. Young's modulus of the SMA layers can be expressed as follows [41]:

$$\begin{aligned}E_1 &= \zeta_1 E_M + (1-\zeta_1)E_A \\ E_3 &= \zeta_3 E_M + (1-\zeta_3)E_A\end{aligned} \tag{17}$$

where E_M and E_A are the martensite and austenite Young's modulus, respectively, and ζ_i $(i = 1,3)$ indicates the martensite fraction for *i*th SMA layer. In this work, a linear model for the phase transformation kinetics presented by Lin and Rogers [42] is implemented. For $M \to A$ transformation with ζ_0, the model is expressed as

$$\begin{aligned}\zeta &= \begin{cases}1 & for\ T \le A_s + |\sigma|/C_A \\ \eta & for\ A_s + |\sigma|/C_A < T < A_f + |\sigma|/C_A \\ 0 & for\ T \ge A_f + |\sigma|/C_A\end{cases} \\ \eta &= 1 - \frac{T - A_s}{A_f - A_s} + \frac{|\sigma|}{C_A(A_f - A_s)}\end{aligned} \tag{18}$$

in which A_s and A_f represent austenite start and austenite final temperatures, respectively, and C_A represents stress-temperature slope for austenite start temperature. In the second temperature interval, ζ is a function of σ and is unknown. In addition, the limits of the temperature intervals are variable and change according to the amount of stress. In this study, it is assumed that in the equilibrium condition of actuator, in each activated SMA layer, only one part of Eq. (18) is satisfied throughout its total length and thickness.

3.1 A, B and D matrixes

Now, by expanding the integrals of the Eq. (15), the following expressions for the stiffness coefficients A, B and D are

$$\begin{aligned}A &= b\left(h_1 E_1 + I_1 + h_3 E_3\right) \\ B &= b\left(E_1\frac{H_2'}{2} + I_2 - E_3\frac{H_2}{2}\right) \\ D &= b\left(E_1\frac{H_3'}{3} + I_3 + E_3\frac{H_3}{3}\right)\end{aligned} \tag{19}$$

in which

$$I_i = \int_{-h_2/2}^{h_2/2} E(z)\,z^{i-1}\,dz \tag{20}$$

and

$$H_2 = \left(\frac{h_2}{2} + h_3\right)^2 - \left(\frac{h_2}{2}\right)^2$$

$$H_2' = \left(\frac{h_2}{2} + h_1\right)^2 - \left(\frac{h_2}{2}\right)^2$$
$$H_3 = \left(\frac{h_2}{2} + h_3\right)^3 - \left(\frac{h_2}{2}\right)^3 \quad (21)$$
$$H_3' = \left(\frac{h_2}{2} + h_1\right)^3 - \left(\frac{h_2}{2}\right)^3$$

where b is width of the beam.

3.2 Mathematical model

Three different factors affect the axial forces and bending moments in the actuator: (1) external loads, (2) thermoelastic stresses induced by temperature changes, and (3) stresses created by phase transformation in SMA layers. Thus, Eq. (11) can be written as follows:

$$N^E = N^M + N^T + N^P = A\varepsilon^0 + B\kappa$$
$$M^E = M^M + M^T + M^P = B\varepsilon^0 + D\kappa \quad (22)$$

Each of three upper indexes M, T and P refer to each three above-mentioned effects. Using Hooke's law for the FGM layer, and the time-independent form of Tanaka and Nagaki's constitutive relation for the SMA layers [43], σ can be determined by the following equations:

$$\sigma = E_2\varepsilon - E_2\alpha\Delta T \quad \text{for FGM layer}$$
$$\sigma = E(\zeta)e + \Theta\Delta T + \Omega(\zeta - 1) \quad \text{for SMA layers} \quad (23)$$

where $\Delta T = T - T_0$, and $e = \varepsilon - \varepsilon_r$ is the relative strain in the SMA layers. Θ and Ω are thermal and phase transformation modules for SMA, respectively. By employing the above constitutive equations, the stress resultants due to temperature change and the phase transformation in SMA layers, can be determined as follows:

$$(N^T, M^T) = \int_{A_1} -\Theta\Delta T_1(1,z)\,dA + \int_{A_2} E_2(z)\alpha(z)\Delta T_2(1,z)\,dA + \int_{A_3} -\Theta\Delta T_3(1,z)\,dA \quad (24)$$

$$(N^P, M^P) = \int_{A_1} \Omega(1-\zeta)(1,z)\,dA + \int_{A_3} \Omega(1-\zeta)(1,z)\,dA \quad (25)$$

where $\Delta T_1 = T_1 - T_0$, $\Delta T_3 = T_3 - T_0$ and $\Delta T_2 = T_2(z) - T_0$, which $T_2(z)$ is defined in Eq. (10). Also, the mechanical stress resultants (N^M,M^M) can be determined by equilibrium equations of the actuator. By expanding the integral of the first part of Eq. (24), the following expressions for the thermal axial force can be written as

$$N^T = \alpha b\left(\frac{1}{h_2}(T_1 - T_3)I_1 + \frac{1}{2}(T_1 + T_3 - 2T_f)I_0\right) - \Theta b((T_1 - T_f)h_1 + (T_3 - T_f)h_3) \quad (26)$$

Similarly, the following expressions are obtained for the thermal bending moment, by integration of the second part of Eq. (24):

$$M^T = \alpha b\left(\frac{1}{h_2}(T_1 - T_3)I_2 + \frac{1}{2}(T_1 + T_3 - 2T_f)I_1\right) - \Theta b((T_1 - T_f)H_2' - (T_3 - T_f)H_2) \quad (27)$$

Substituting Eq. (18) into the first part of Eq. (25), and noting that the upper and lower SMA layers can be activated with two different input loads, the following expressions for the phase transformation axial force can be obtained:

$$N^P = N_1^{Pi} + N_3^{Pk} \quad (i = 1or2or3), \quad (k = 1or2or3) \quad (28)$$

where, N_1^{pi} and N_3^{pk} are given in Eq. (29). The superscripts i and k are referred to one of the three temperature intervals in Eq. (18).

$$\begin{cases} N_1^{P1} = 0 \\ N_1^{P2} = \Lambda_1\varepsilon^0 + \Delta_1\kappa + \Gamma_1 \\ N_1^{P3} = \Omega b h_1 \end{cases} \quad (29\text{-a})$$

$$\begin{cases} N_3^{P1} = 0 \\ N_3^{P2} = \Lambda_3\varepsilon^0 + \Delta_3\kappa + \Gamma_3 \\ N_3^{P3} = \Omega b h_3 \end{cases} \quad (29\text{-b})$$

where, the coefficients Λ_1, Δ_1 and Γ_1 are given by

$$\Lambda_1 = -\frac{jE_1 bh_1\Omega}{C_A(A_f - A_s) - j\Omega}$$
$$\Delta_1 = -\frac{jE_1 L_1\Omega}{C_A(A_f - A_s) - j\Omega} \quad (30\text{-a})$$
$$\Gamma_1 = \left[\frac{C_A(T_1 - A_s) - j\Theta\Delta T_1}{C_A(A_f - A_s) - j\Omega}\right] bh_1\Omega \quad (30\text{-b})$$

In the above equations $j = \mathrm{sgn}(\sigma)$ represents the sign of stress in the SMA layer. The coefficients Λ_3, Δ_3, and Γ_3 are determined by similar expressions, except that T_1, h_1 and L_1 should be replaced by T_3, h_3 and L_3 respectively. Similarly, for the phase transformation bending moment, M^P, one has

$$M^P = M_1^{Pi} + M_3^{Pk}$$
$$(i = 1 or\ 2 or\ 3), \qquad (k = 1 or\ 2 or\ 3) \quad (31)$$

in that

$$\begin{cases} M_1^{P1} = 0 \\ M_1^{P2} = \Lambda_1'\varepsilon^0 + \Delta_1'\kappa + \Gamma_1' \\ M_1^{P3} = \Omega L_1 \end{cases} \quad (32\text{-a})$$

$$\begin{cases} M_3^{P1} = 0 \\ M_3^{P2} = \Lambda_3'\varepsilon^0 + \Delta_3'\kappa + \Gamma_3' \\ M_3^{P3} = \Omega L_3 \end{cases} \quad (32\text{-b})$$

where

$$\Lambda_1' = -\frac{jE_1 L_1\Omega}{C_A(A_f - A_s) - j\Omega}$$
$$\Delta_1' = -\frac{jE_1 I_1\Omega}{C_A(A_f - A_s) - j\Omega} \quad (33\text{-a})$$
$$\Gamma_1' = \left[\frac{C_A(T_1 - A_s) - j\Theta\Delta T_1}{C_A(A_f - A_s) - j\Omega}\right] L_1\Omega \quad (33\text{-b})$$

Expressions for Λ_3', Δ_3', and Γ_3' are the same as those for Λ_1', Δ_1', and Γ_1' presented by Eq. (33), except that T_1, h_1 and L_1 should be replaced by T_3, h_3 and L_3 respectively. If the martensitic residual strain, ε_r, initially constituted in the SMA layers is less than the recovery strain limit, ε_L, in Eqs. (29)-(33), Ω should be replaced by a corrected value Ω_c, which can be computed from $\Omega_c = \Omega\varepsilon_r / \varepsilon_L$. In Eqs. (28) and (31), N^P, M^P can be represented by general expressions as follows:

$$N^P = \Lambda\varepsilon^0 + \Delta\kappa + \Gamma$$
$$M^P = \Lambda'\varepsilon^0 + \Delta'\kappa + \Gamma' \quad (34)$$

where

$$\Lambda = \Lambda_1 + \Lambda_3; \quad \Delta = \Delta_1 + \Delta_3; \quad \Gamma = \Gamma_1 + \Gamma_3$$
$$\Lambda' = \Lambda_1' + \Lambda_3'; \quad \Delta' = \Delta_1' + \Delta_3'; \quad \Gamma' = \Gamma_1' + \Gamma_3' \quad (35)$$

Here, for each of the heated SMA layers, in the first and third temperature intervals of Eq. (18), the coefficients Λ, Δ and Λ', Δ' are equal to zero. As can be seen in Eq. (34), the force and moment due to phase transformation are functions of ε^0, κ. This indicates nonlinearity in the actuator behavior. In this study, a linear approximation is presented. After determining the mechanical, thermal and phase transformation forces and moments, and their substitution into Eq. (22), Eq. (34) is derived, which can be solved simultaneously for ε^0, κ

$$\begin{aligned} N^E &= N^M + N^T + (\Lambda\varepsilon^0 + \Delta\kappa + \Gamma) \\ &= A\varepsilon^0 + B\kappa \\ M^E &= M^M + M^T + (\Lambda'\varepsilon^0 + \Delta'\kappa + \Gamma') \\ &= B\varepsilon^0 + D\kappa \end{aligned} \quad (36)$$

Rearranging of Eq. (36), one has

$$\varepsilon^0 = \Psi^{-1}\begin{vmatrix} N^M + N^T + \Gamma & B - \Delta \\ M^M + M^T + \Gamma' & D - \Delta' \end{vmatrix}$$
$$\kappa = \Psi^{-1}\begin{vmatrix} A - \Delta & N^M + N^T + \Gamma \\ B - \Delta' & M^M + M^T + \Gamma' \end{vmatrix} \quad (37)$$

where

$$\Psi = (A - \Lambda)(D - \Delta') - (B - \Delta)(B - \Lambda') \quad (38)$$

Eq. (37) can be solved for midplane strain and curvature of the actuator. Finally, the axial midplane displacement u_2 and lateral deflection w of the actuator can be determined by solving Eq. (13).

4. Numerical results and discussion

In order to solve the above relations, in this section, an SMA bonded FG beam (as shown in Fig. 1) is considered under clamped-free boundary condition. The length (*L),* width (*b)* and the thickness of the FG core are 200 mm, 30 mm and 1.5 mm, respectively, and the SMA layers are considered to have the same thickness, $h_1 = h_3$. Thickness ratio of the SMA layers to the FG core layer is 0.2.

For the procedure outlined above, a code was developed in MATLAB workspace. This program is executed for computing the behavior of the beam shown in Fig. 1, with the physical properties listed in Tables 1 and 2. The values of the physical properties are for Nitinol as the SMA layers and Aluminium-Ceramic as the core FG layer. In this example, only the upper SMA layer is considered to be activated, $T_1 > T_3 = T_0$. Estimating ε^0 and κ as one degree functions of x

$$\varepsilon^0 = C_1\bar{x} + C_2 \; ; \quad \bar{\kappa} = C_3\bar{x} + C_4 \tag{39}$$

and then integrating according to Eq. (13) gives

$$\bar{u}^0 = C_1'\bar{x}^2 + C_2'\bar{x} \; ; \; \bar{w} = C_3'\bar{x}^3 + C_4'\bar{x}^2 \tag{40}$$

C_i' $(i = 1,2,3,4)$ are functions of the FGM volume fraction index, activation temperature, thicknesses, elastic modulus of metal and ceramic, slope of the FGM. Elastic modulus changes with respect to temperature, and martensitic residual strain in the SMA layers.

The effect of each of the above-mentioned parameters on the actuator displacements response was examined under a non-dimensional loading of $\bar{p} = p / h_2^2 = 1$. The results are illustrated in Figs. 2-7. Fig. 2 shows the effect of activation temperature T_1 on non-dimensional deflection $\bar{w}$ and Fig. 3 shows the effect of activation temperature T_1 on non-dimensional displacement $\bar{u}_0$. T_3 is assumed to be *300K* and the beam is considered to be fully ceramic ($g = \infty$ *)*. One can see a significant deflection during phase transformation.

The effects of thickness of FGM layer on the actuator responses are shown in Figs. 4 and 5. Substantial nonlinear change in displacements can occur as this parameter is varied. In these figures, no phase transformation is considered and the SMA layers are assumed to be fully martensitic. Increasing the FGM layer thickness results in a significant decrease in lateral deflection, while the axial displacement keeps its trend to increase in absolute magnitude.

In the next step, we investigate the effect of the FGM power index, *g*, on the displacements of the compound beam. The obtained results in Fig. 6 and Fig. 7 indicate that by increasing the value of *g*the lateral deflection decreases, while the axial displacement of the system increases when 300K activation temperature is applied. Moreover, as it is shown in Table 3, this decreasing trend of $\bar{w}$ and increasing trend of $\bar{u}_0$ for smaller values of FGM index is more pronounced. For example, in the case of a beam under 300k activation temperature, by increasing the value of *g* from 0.1 to 1 (about 1000%), the axial deformation for the compound beam increases by 25.75%, but by increasing *g* from 1 to 10 (about 1000%) of the same beam and for the same activation temperature, it increases by 20.49%. Similarly, 25.73% and 20.46% decrease can be seen for lateral deflection. This can be seen better in the Figs. 8 and 9.

Table 1. Material properties for a Nitinol alloy [44].

Module/Density	Transformation Temperatures	Transformation Constants	Other	
E_a=67 x 103 Mpa	M_f=9 ºC	C_M =8 Mpa/ ºC	Max. Residual strain	ε_L = 0.067
E_m=26.3 x 103 Mpa	M_s=18.4 ºC	C_A = 13.8 Mpa/ ºC	Resistivity	ρ_e = 0.9 x 10-6
θ =0.55 Mpa/oC	A_s=34.5 ºC	σ_s^{cr} =100 Mpa	Specific heat	C_p = 920 J/kg oC
ρ =6500 kg/m3	A_f=49 ºC	σ_f^{cr} = 170 Mpa	Conductivity	χ = 18 W/m oC

Table 2. Material properties and geometry of FGM core beam (Subscript *c* indicates Ceramic and subscript *m* indicates Aluminum as metal).

E_c (GPa)	E_m (GPa)	ρ_c (kg m^{-3})	ρ_m (kg m^{-3})	Poison's ratio
205	70	8900	7000	0.3

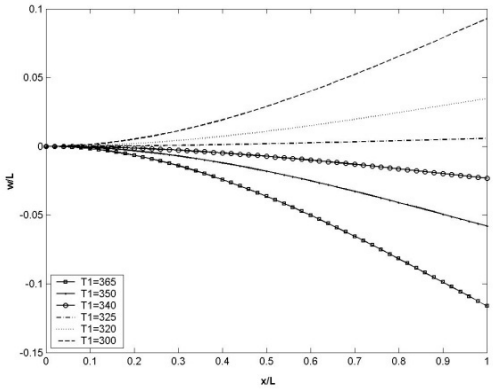

Fig. 2. The effect of activation temperature (K), T_1, on the non-dimentional lateral deflection (w/L) of the actuator beam (h_2/L=7.5e-3, $h_1/h_2=h_3/h_2$=0.2, $g=\infty$).

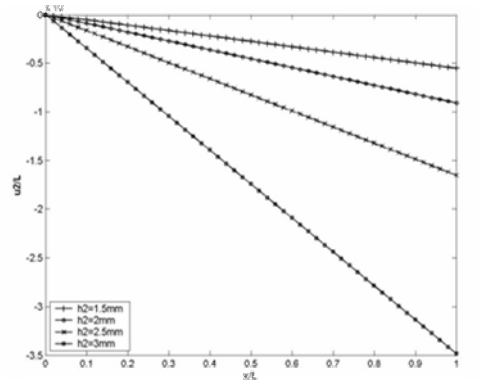

Fig. 5. The effect of FGM layer thickness, h_2, on the non-dimensional axial deflection (u_2/L) of the actuator beam (T_1=300k, $g=\infty$).

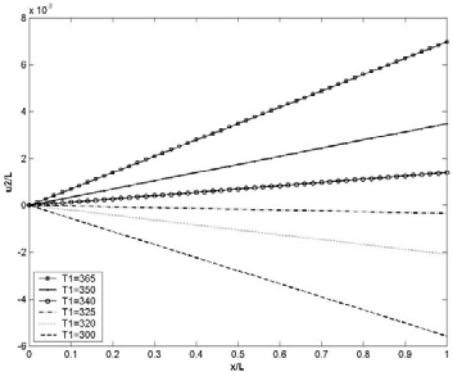

Fig. 3. The effect of activation temperature (K), T_1, on the non-dimensional axial deflection (u_2/L) of the actuator beam (h_2/L=7.5e-3, $h_1/h_2=h_3/h_2$=0.2, $g=\infty$).

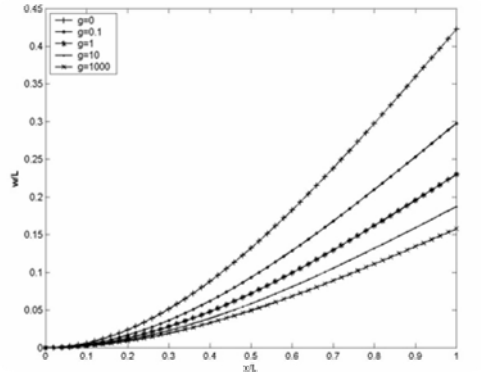

Fig. 6. The effect of FGM index, g, on the non-dimensional lateral deflection (w/L) of the actuator beam (T_1=300k).

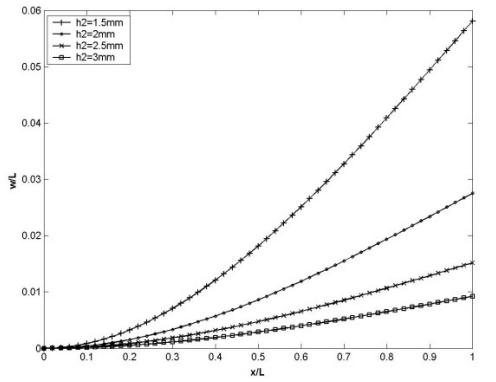

Fig. 4. The effect of FGM layer thickness, h_2, on the non-dimensional lateral deflection (w/L) of the actuator beam (T_1=300k, $g=\infty$).

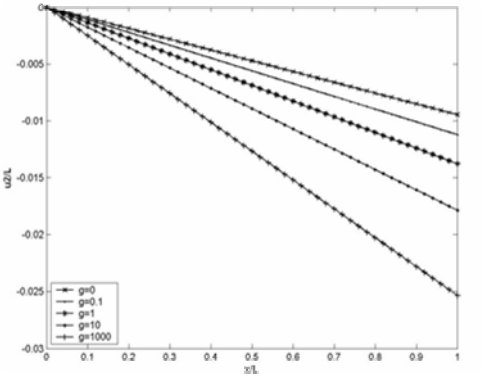

Fig. 7. The effect of FGM index, g, on the non-dimensional axial deflection (u_2/L) of the actuator beam (T_1=300k).

Table 3. The effect of FGM index to the tip deflection of the actuator beam (h_2/L=7.5e-3, $h_1/h_2=h_3/h_2$=0.2).

g	T_1 (k)	w (L)/L	u_2 (L)/L	g	T_1 (k)	w (L)/L	u_2 (L)/L
0	300	0.67588	-0.04055	0.1	300	0.47626	-0.02858
	325	0.042242	-0.00253		325	0.029766	-0.00179
	365	-0.84485	0.050691		365	-0.59532	0.035719
0.001	300	0.64351	-0.03861	1	300	0.36766	-0.02206
	325	0.040219	-0.00241		325	0.022979	-0.00138
	365	-0.80439	0.048263		365	-0.45958	0.027575
0.01	300	0.57883	-0.03473	10	300	0.2994	-0.01796
	325	0.036177	-0.00217		325	0.018712	-0.00112
	365	-0.72354	0.043412		365	-0.37425	0.022455

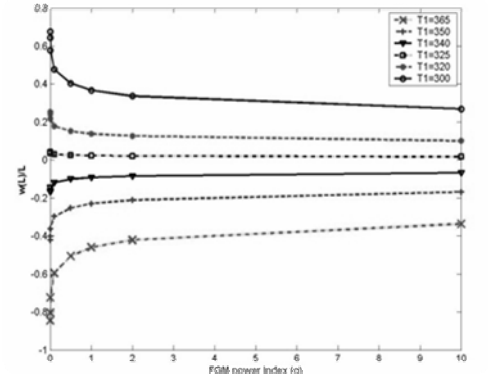

Fig. 8. non-dimensional lateral deflection for the tip of the actuator beam (h_2/L=7.5e-3, $h_1/h_2=h_3/h_2$=0.2).

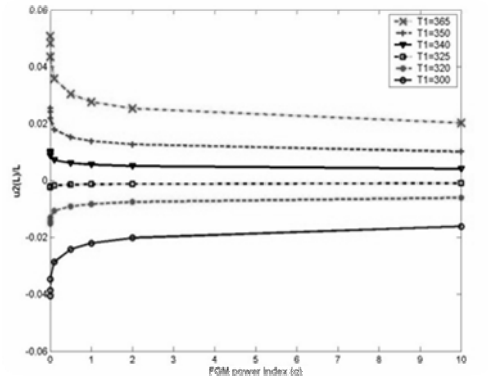

Fig. 9. non-dimensional axial displacement for the tip of the actuator beam (h_2/L=7.5e-3, $h_1/h_2=h_3/h_2$=0.2).

5. Conclusion

A theoretical study of the thermally driven behavior of an SMA/FGM actuator under arbitrary loading and boundary conditions was presented by developing an integrated mathematical model. The constitutive equation and linear phase transformation kinetics relations of SMA layers depicted by Tanaka and Nagaki are coupled with the governing equation of the actuator to predict the stress history in smart SMA/FGM beam and to model the thermomechanical behavior. Based on the classical laminated beam theory, the explicit solution to the structural response of the structure, including axial and lateral deflections of the structure, is investigated. As an example, a cantilever box beam with uniform square cross-section subjected to a transverse concentrated load is solved numerically. The effect of some factors such as activation temperature, FGM layer thickness and FGM index factor is investigated and showed diagrammatically. It can be inferred from the results that the deflection during phase transformation is significant and increasing the FGM layer thickness results in decreasing the lateral deflection, while the axial displacement keeps its trend to increase in absolute magnitude. The obtained results also indicate that by increasing the value of g the lateral deflection decreases, while the axial displacement of the system increases when 300K activation temperature is applied. Moreover, decreasing trend of and increasing trend of for smaller values of FGM index are more pronounced.

References

[1] M. Koizumi, The concept of FGM, *Ceram. Trans. Funct. Grad. Mater.* 34 (1993) 3-10.

[2] M. Teymur, N. R. Chitkara, K. Yohngjo, J. Aboudi, M. J. Pindera and S. M. Arnold, Thermoelastic theory for the response of materials functionally graded in two directions, *Int. J. Solids Struct.* 33 (1996) 931-66.

[3] E. Feldman and J. Aboudi, Buckling analysis of

functionally graded plates subjected to uniaxial loading, *Compos. Struct.* 38 (1997) 29-36.

[4] B. V. Sankar, An elasticity solution for functionally graded beams, *Compos. Sci. Technol.* 61 (2001) 689-96.

[5] R. C. Batra and S. S. Vel, Exact solution for thermoelastic deformations of functionally graded thick rectangular plates, *AIAA J.* 40 (2001) 1421-33.

[6] Z. Zhong and E. T. Shang, Three dimensional exact analysis of a simply supported functionally gradient plate, *Int. J. Solids Struct.* 40 (2003) 5335-52.

[7] C. T. Loy, K. Y. Lam and J. N. Reddy, Vibration of functionally graded cylindrical shells, *Int. J. Mech. Sci.* 41 (1999) 309-24.

[8] J. Yang and H. S. Shen, Dynamic response of initially stressed functionally graded rectangular thin plates, *Compos. Struct.* 54 (2001) 497-508.

[9] J. Woo and S. A. Meguid, Nonlinear analysis of functionally graded plates and shallow shells, *Int. J. Solids Struct.* 38 (2001) 7409-21.

[10] H. S. Shen, Nonlinear bending response of functionally graded plates subjected to transverse loads and in thermal environments, *Int. J. Mech. Sci.* 44 (2002) 561-84.

[11] M. Aydogdu and V. Taskin, Free vibration analysis of functionally graded beams with simply supported edges, *Materials and Design* 28 (2007) 1651-1656.

[12] Z. Zhong and T. Yu, Analytical solution of a cantilever functionally graded beam, *Composites Science and Technology* 67 (2007) 481-488.

[13] S. A. Sina, H. M. Navazi and H. Haddadpour, An analytical method for free vibration analysis of functionally graded beams, *Materials and Design* 30 (2009) 741-747.

[14] X. Gao, M. Huang and L. C. Brinson, A multivariant micromechanical model for SMAs Part 1. Crystallographic issues for single crystal model, *International Journal of Plasticity*, 16 (2000) 1345-1369.

[15] X. Gao, M. Huang and L. C. Brinson, A multivariant micromechanical model for SMAs Part 2. Polycristal model, *International Journal of Plasticity*, 16 (2000) 1345-1369.

[16] Xiujie Gao and L. Catherine Brinson, A Simplified Multivariant SMA Model Based on Invariant Plane Nature of Martensitic Transformation, *Northwestern University*, Technical Notes.

[17] L. C. Brinson, A. Bekkrer and S. Hwang, Deformation of Shape Memory Alloy Due to Thermo-Induced Transformation, *J. of Intell. Mater. Syst. Struct.*. 7, Jan., 97-107.

[18] L. C. Brinson and R. Lammering, Finite element analysis of the behavior of shape memory alloys and their applications, *Int. J. Solids Structures,* 30 (23) (1993) 3261-3280.

[19] M. Brocca, L. C. Brinson and Z. P. Bazant, Three Dimensional Constitutive Model for Shape Memory Alloys Based on Microplane Model, *J. Mech. Phys. Solids*, 1999.

[20] F. Ebrahimi and A. Rastgoo, 2008a Free vibration analysis of smart annular FGM plates integrated with piezoelectric layers, *Smart Mater. Struct*, 17 No. 015044 13 pp, doi: 10.1088/0964-1726/17/1/015044.

[21] F. Ebrahimi and A. Rastgoo and M. H. Kargarnovin, 2008a Analytical investigation on axisymmetric free vibrations of moderately thick circular functionally graded plate integrated with piezoelectric layers, *Journal of Mechanical Science and Technology* 22 (16) 1056-1072.

[22] F. Ebrahimi, A. Rastgoo and A. A. Atai, 2008b, Theoretical analysis of smart moderately thick shear deformable annular functionally graded plate, *European Journal of Mechanics - A/Solids*, published online: 25 Dec. (2008).

[23] D. C. Lagoudas, J. G. Boyd and Z. Bo, Micromechanics of active composites with SMA fibers, Trans. ASME, *Eng. Mat. Tech.* 116 337 (1994).

[24] M. Kawai, H. Ogawa, V. Baburaj and T. Koga, Micromechamical Analysis for Hysteretic Behavior of Unidirectional TiNi SMA Fiber Composites, *J. Intell. Mater. Struct.* 10 14 (1999).

[25] G. Murasawa, K. Tohgo and H. Ishii, Deformation Behavior of NiTi/Polymer Shape Memory Alloy Composites – Experimental Verifications, *J. Compos. Mater.* 38 399 (2004).

[26] S. M. R. Khalili, A. Shokuhfar, K. Malekzadeh and F. A. Ghasemi, Low-velocity impact response of active thin-walled hybrid composite structures embedded with SMA wires, *Thin-Walled Structures* 45 (2007) 799-808.

[27] S. M. R. Khalili, A. Shokuhfar and F. A. Ghasemi, Effect of smart stiffening procedure on low-velocity impact response of smart structures, *Journal of Materials Processing Technology* 190 (2007) 142-152.

[28] H. Sepiani and A. Ghazavi, A thermo-micromechanical modeling for smart shape memory alloy woven composite under in-plane biaxial deformation, *Int J Mech Mater Des*, DOI 10.1007/s10999-008-9088-9.

[29] G. Zhou, L. M. Sim, P. A. Brewster and A. R. Giles, Through-the-thickness mechanical properties of smart quasi-isotropic carbon/epoxy laminates, *Composites: Part A* 35 (2004) 797-815.

[30] M.-L. Dano and M. W. Hyer, SMA-induced snap-through of unsymmetric fiber-reinforced composite laminates, *International Journal of Solids and Structures* 40 (2003) 5949-5972.

[31] M. M. ghomshei, N. Tabandeh, A. Ghazavi and F. Gordaninejad, A three-dimensional shape memory alloy/elastomer actuator, *Composites: Part B* 32 (2001) 441-449.

[32] M. M. ghomshei, N. Tabandeh, A. Ghazavi and F. Gordaninejad, Nonlinear transient response of a thick composite beam with shape memory alloy layers, *Composites: Part B* 36 (2005) 24-9.

[33] B. S. Balapgol, K. M. Bajoria and S. A. Kulkarni, Natural frequencies of a multilayer SMA laminated composite cantilever plate, *Smart Mater. Struct.* 15 (2006) 1021-1032.

[34] Q. Chen and C. Levy, Active vibration control of elastic beam by means of shape memory alloy layers, *Smart Mater. Struct.* 5 (1996) 400-406.

[35] A. J. Markworth, K. S. Ramesh and W. P. Parks Jr. Modeling studies applied to functionally graded materials, *J. Mater. Sci.* 30 (1995) 2183-93.

[36] J. N. Reddy and G. N. Praveen, Nonlinear transient thermoelastic analysis of functionally graded ceramic-metal plate, *Int. J. Solids Struct.* 35 (1998) 4457-76.

[37] R. C. Wetherhold, S. Seelman and S. Wang, The use of functionally graded materials to eliminate or control thermal deformation, *Compos. Sci. Technol.* 56 (1996) 1099-104.

[38] Y Tanigawa, H. Morishita and S. Ogaki, Derivation of system of fundamental equations for a three dimensional thermoelastic field with nonhomogeneous material properties and its application to a semi infinite body, *J. Therm. Stresses* 22 (1999) 689-711.

[39] K. Ikuta and H. Shimizu, Two-dimensional mathematical model of shape memory alloy and intelligent SMA-CAD MEMS: *Proc. IEEE Micro Electro Mechanical System* (Piscataway, NJ: IEEE) (1993) 87-92.

[40] R. F. Gibson, Principles of composite material mechanics. New York: *McGraw-Hill*, (1994).

[41] D. C. Lagoudas, J. G. Boyd and B. Bo, Analysis of a coupling made of shape memory alloy and its dynamic response due impacts, J. *Vibration Acoustics* 114 (1992) 297-304.

[42] M. W. Lin and C. A. Rogers, Analysis of stress distribution in a shape memory alloy composite beam, *AIAA*-91-1164-CP (1991).

[43] K. Tanaka and S. Nagaki, Thermomechanical description of material with internal variables in the process of phase transformation, *Ingenieur Archiv,* 51 (1982) 287-99.

[44] L. C. Brinson, One dimensional constitutive behavior of shape memory alloys: thermomechanical derivation with nonconstant material functions, *Journal of Intelligent Material Systems and Structures* 4 (2) (1993) 229-242.

Hossein Ali Sepiani received his B.S. in Mechanical Engineering from the University of Kashan, Iran, in 2003. He then received his M.S. degree from the University of Tehran, in 2006. Currently, Hossein is continuing his research at the University of Tehran. His research interests include new materials (FGMs, Nano-materials, SMAs, SMPs, etc.), composites (Woven Fabrics and Fiber Metal Laminates), smart materials (Shape Memory Alloy, Magnet/Electro-rheological and Piezoelectric Sensors and Actuators), intelligent structures (Structures integrated with smart materials), vibration and control of intelligent structures and their application.